Splitting-scheme Solution of the Collisionless Wigner Equation with Non-Parabolic Band Profile

Lucio Demeio [1]

Abstract

In this work, we present a numerical application of a recently developed transport model for semiconductors, based on the Wigner-function approach and allowing for non-parabolic band profiles. We consider the collisionless, single-band time evolution of the Wigner function under the action of a constant external field, in presence of a band profile exhibiting a satellite valley, besides the minimum at the center of the Brillouin zone (similar to the band profile of GaAs). The transport equation is solved by the Splitting-Scheme algorithm, which is the most efficient method for solving the correspinding classical Vlasov equation.

Key-words: Wigner function, Semiconductors, Quantum Transport, Non-parabolic Electron Transport.

[1] Dipartimento di Scienze Matematiche, Università Politecnica delle Marche, Via Brecce Bianche 1, 60131 Ancona - Italy, e-mail: demeio@mta01.univpm.it

1 Introduction

In the study of the transport properties of semiconductors and electronic devices, Wigner functions are commonly used for the statistical description of carrier ensembles and of their dynamics [1, 2]. For the most part, however, only those processes which can be adequately described within the single-band and the parabolic-band approximations are considered. In order to generalize the Wigner-function approach to those situations in which these approximations are not satisfactory, a general multi-band transport model was recently developed in [3, 4] (see also [5]), where a multi-band Wigner function was introduced and the evolution equation allowed for energy bands of arbitrary shape.

In this contribution, we investigate numerically the single-band time evolution of an initial Gaussian shaped Wigner function describing an ensemble of conduction electrons moving under the action of an external field and in the presence of a non-parabolic band profile. The numerical solution is obtained with the Splitting-Scheme algorithm, which is described in Section 3.

2 The Non-Parabolic Transport Model

The Wigner function is defined by a suitable Fourier transformation of the density matrix [6, 7]. Let $\rho(r,s) =< r|\rho|s >$ be the single-particle density matrix in the space representation. Then, the corresponding single-particle Wigner function is defined by

$$f(x,p) = \int d\eta < x + \frac{\eta}{2}|\rho|x - \frac{\eta}{2} > e^{-ip\eta/\hbar}, \tag{1}$$

together with its inverse

$$< r|\rho|s >= \frac{1}{2\pi\hbar}\int dp f\left(\frac{r+s}{2}, p\right) e^{ip(r-s)/\hbar}. \tag{2}$$

Usually, $x = (r+s)/2$ is identified with a center of mass variable and $\eta = r - s$ with a relative position variable.

The single-band evolution equation of the Wigner function of an ensemble of conduction electrons moving in a semiconductor medium, in the presence of an arbitrary band profile and under the action of an external potential, is given by [4, 8]

$$\frac{\partial f}{\partial t}(x,p,t) + (Af)(x,p,t) + (\Theta f)(x,p,t) = 0, \tag{3}$$

where the transport operator A and the pseudodifferential operator Θ are defined by

$$(Af)(x,p,t) = \frac{i}{\hbar}\sum_{\mu\in L}\widehat{\epsilon}(\mu)\left[f(x+\frac{\mu}{2},p,t) - f(x-\frac{\mu}{2},p,t)\right]e^{ip\mu/\hbar}$$

$$(\Theta f)(x,p,t) = \frac{i}{\hbar}\int d\eta\delta V(x,\eta)\widehat{f}(x,\eta,t)e^{-ip\eta/\hbar}.$$

Here, $\widehat{f}(x,\eta,t)$ is the Fourier transform of the Wigner function with respect to the momentum variable, $\widehat{\epsilon}(\mu)$, $\mu\in L$, are the Fourier coefficients of the energy band and $\delta V(x,\eta) = V(x+\eta/2) - V(x-\eta/2)$ is the symbol of the pseudodifferential operator, with $V(x)$ the external potential. The action of the periodic potential is described by the first term, which contains the Fourier coefficients of the energy band, and which reduces to the usual free-streaming operator in the parabolic-band approximation. The second term describes the action of the external potential.

3 The Splitting-Scheme Algorithm

Usually, the time-dependent or stationary transport equations that govern the behaviour of the Wigner function are solved numerically by finite difference techniques [1]. In the numerical solution of the classical transport equations, and more specifically of the Vlasov equation, the most efficient method is the Splitting-Scheme algorithm [9]. A quantum version of the Splitting-Scheme algorithm was introduced in [10, 11] for the case of a parabolic energy-momentum dispersion relation; we now briefly describe our generalization to the non-parabolic case.

For the numerical solution of Eq. (3), we discretize the time variable with $t_n = t_{n-1}+\Delta t$, $t_0 = 0$ and indicate with $f_n(x,p) = f(x,p,t_n)$ the discretized Wigner function. Suppose, now, that $f_n(x,p)$, the Wigner function at the time $t = t_n$, is known. Then, the Splitting Scheme integration from time t_n to time t_{n+1} is given by the following sequence of operations:

- (step 1): first, the equation

$$\frac{\partial g_1}{\partial t} + Ag_1 = 0 \tag{4}$$

  is solved for $g_1(x,p,t)$ from $t = 0$ to $t = \Delta t/2$, with initial condition $g_1(x,p,0) = f_n(x,p)$;

- (step 2): then, the equation

$$\frac{\partial g_2}{\partial t} + \Theta g_2 = 0 \tag{5}$$

  is solved for $g_2(x,p,t)$ from $t = 0$ to $t = \Delta t$, with initial condition $g_2(x,p,0) = g_1(x,p,\Delta t/2)$;

- (step 3): finally, the equation

$$\frac{\partial g_3}{\partial t} + A g_3 = 0 \tag{6}$$

  is solved again for $g_3(x,p,t)$ from $t = 0$ to $t = \Delta t/2$, with initial condition $g_3(x,p,0) = g_2(x,p,\Delta t)$.

The Wigner function at the time t_{n+1} is then given by $f_{n+1}(x,p) = g_3(x,p,\Delta t/2)$. When the self-consistent field is not taken into account, the steps 1 and 3 can be combined into a single step, as we do in the numerical example presented here; otherwise, the self-consistent field is calculated at the end of step 1, which makes the Splitting Scheme a second-order algorithm in Δt. For the classical Vlasov equation, the Splitting-Scheme performes an integration along the phase-space characteristics. In that case, steps 1 and 3 correspond to a shift in the x direction, while step 2 corresponds to a shift in the p direction.

Equations (4), (5) and (6) can be solved explicitely. Equation (4) can be solved by using Fourier transforms in space. If $\widehat{g_1}_k$ is the $k-$th Fourier component of g_1 with respect to x, it is easy to see that

$$\widehat{g_1}_k(p,t) = \widehat{g_1}_k(p,0) e^{i\gamma_k(p)t}$$

where $\gamma_k(p) = 2i \sum_\mu \widehat{\epsilon}(\mu) \sin(k\mu/2) \exp(ip\mu/\hbar)$. A similar result holds for $G(x,p,t)$ in equation (6). Equation (5) can be solved by using Fourier transforms in momentum. If $\widetilde{g_2}(x,\eta,t)$ is the Fourier Transform of g_2 with respect to p, we have that

$$\widetilde{g_2}(x,\eta,t) = \widetilde{g_2}(x,\eta,0) e^{-i\delta V(x,\eta)t/\hbar}.$$

4 Numerical results

In this example, we study the time evolution of the Wigner function of an ensemble of electrons under the action of a constant external field and in presence of a non-parabolic band profile. We use the model of Section

2 and solve numerically equation (3) with the Splitting-Scheme algorithm described in Section 3. We have chosen a band profile somewhat similar to the band profile of GaAs, with a minimum at $k = 0$ a second minimum at about half of the Brillouin zone. The band shape, shown in Figure 1, is given by the finite Fourier expansion

$$\epsilon(k) = \sum_{\mu \in L} \widehat{\epsilon}_m(\mu) e^{ik\mu},$$

with $\mu = la$ and $\widehat{\epsilon}(\mu) = b_l e^{i\phi_l}$. Here, $b_0 = 2$ eV, $b_1 = -0.05$ eV, $b_2 = -0.05$ eV and $b_3 = 0.25$ eV, $b_l = 0$, $l > 3$ and $\phi_l = 0$, $l = 0, \ldots$. Also, we take $a = 5.65\ 10^{-8}$ cm (GaAs lattice period).

The external field acts on a spatial region slightly smaller than the simulation region and is derived from the potential energy

$$V(x) = \begin{cases} V_0, & x \leq -L_1 \\ (V_0/2)(1 - x/L_1), & -L_1 \leq x \leq L_1 \\ 0, & x \geq L_1. \end{cases}$$

Moreover, we impose the boundary conditions $f(x, p_{max}) = f(x, -p_{max}) = 0$, with $p_{max} = \hbar\pi/a$, and $f(-L, p) = f(L, p) = 0$, that is the we assume that the Wigner function vanishes at the boundary of the simulation region. In this simulation, we have taken $L = 100\ a$ $L_1 = 0.8\ L$ and $V_0 = 5$ eV.

The initial Wigner function (shown in Figure 2) corresponds to a pure state characterized by the wave function

$$\Psi(x) = e^{-(\alpha^2/2)(x-x_0)^2} e^{-ik_0(x-x_0)},$$

where x_0 is the initial average position, k_0 the initial average momentum and α the initial momentum spread. The density matrix is then given by $\rho(x, x') = \Psi(x)\Psi^*(x')$ and the Wigner function that results is

$$f(x, p, 0) = 2e^{-(\alpha^2/2)(x-x_0)^2 - (p-\hbar k_0)^2/(\alpha\hbar)^2},$$

where the normalization $||f|| = \int\int f(x, p)dx\ dp = 1$ has been used. In this example we have $x_0 = -0.6\ L$, $k_0 = 0$ and $\alpha = 0.04\ \pi/a$.

The time evolution of the Wigner function is shown in Figures 2 (initial state), 3, 4 and 5, at $t = 0$, 12, 28 and 40 fs, respectively. On the floor of the boxes, the graph of the band profile (in the p variable) is also shown for reference. The initial Wigner distribution describes a group of electrons near the central minimum of the band. Initially, the Wigner function evolves according to a free-streaming law, consistent with the parabolic-band approximation (see Figure 3). Subsequently, as the portions of the Wigner

distribution enter the region where the band profile decreases, they suffer a deceleration and the Wigner function is pushed back, as can be seen from Figure 4. Eventually, as the centroid of the Wigner function reaches the secondary minimum (at about $t = 40$ fs on this example, see Figure 5), the Wigner function approximately resumes the initial shape.

References

[1] W. R. Frensley, *Rev. Modern Phys.*, **62**:745-791 (1990).

[2] C.Jacoboni, R.Brunetti, P. Bordone, and A. Bertoni, Quantum transport ans its simulation with the Wigner-function approach, in *Topics in High Field Transport in Semiconductors*, K. Brennan and P.Paul Ruden, ed. (World Scientific, Singapore 2001), pp.25-61.

[3] L. Demeio, L. Barletti, A. Bertoni, P. Bordone and C. Jacoboni, *Physica B*, **314**:104-107 (2002).

[4] L. Demeio, P. Bordone and C. Jacoboni, Multi-band, non-parabolic Wigner-function approach to electron transport in semiconductors, Internal Report, Quaderno N. 3/2003 (Dipartimento di Scienze Matematiche, Università Politecnica delle Marche, April 2003, submitted to the J. of Stat. Phys.)

[5] G. Borgioli, G. Frosali and P.F. Zweifel, Proc. XVII International Conference on Transport Theory, London, July 2001, in *Transport Theory Stat. Phys.*, in press.

[6] E. Wigner, *Phys. Rev.*, **40**:749-759 (1932).

[7] P. A. Markowich, C. A. Ringhofer and C. Schmeiser, *Semiconductor Equations* (Springer-Verlag, Wien 1990).

[8] P. A. Markowich, N. J. Mauser and F. Poupaud, *J. Math. Phys.*, **35**:1066-1094 (1994).

[9] C. G. Cheng and G. Knorr, *J. Computat. Phys.* **22**:330-351 (1976).

[10] A. Arnold and C. Ringhofer, *SIAM J. of Num. Anal.* **32**: 1876-1894 (1995).

[11] A. Arnold and C. Ringhofer, *SIAM J. of Num. Anal.* **33**: 1622-1643 (1996).

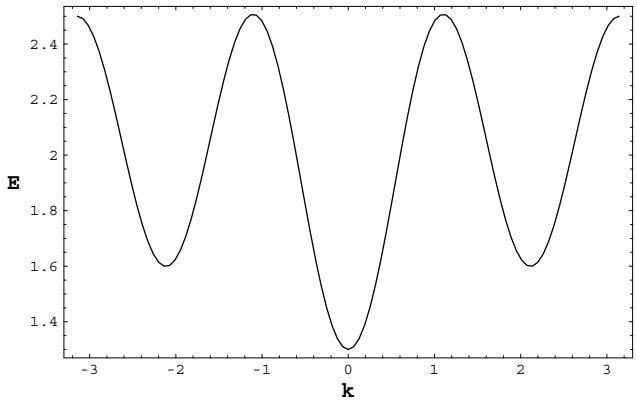

Figure 1: Band profile $\epsilon(k)$ in eV, $-\pi \leq ka \leq \pi$.

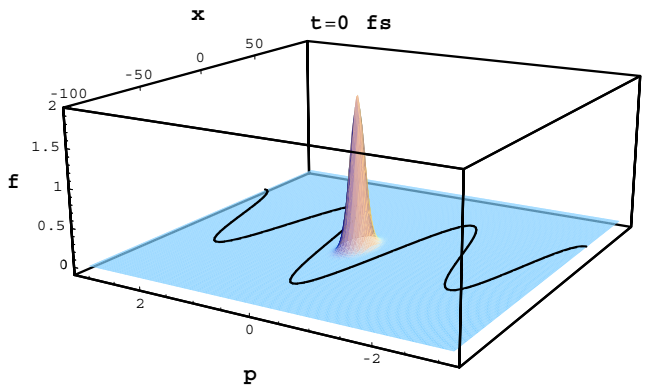

Figure 2: $f(x,p,t)$ at $t = 0$ (initial Wigner distribution), $-100 \leq x \leq 100$, $-\pi \leq p \leq \pi$.

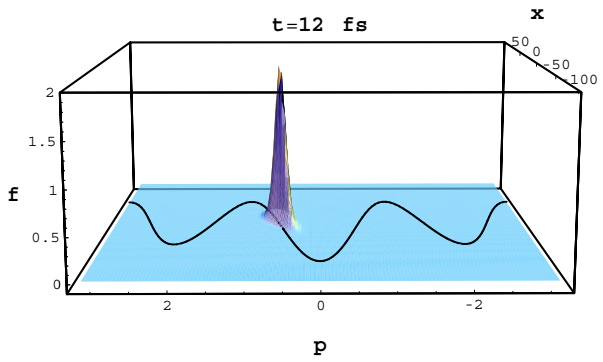

Figure 3: $f(x,p,t)$ at $t = 12$ fs, $-100 \leq x \leq 100$, $-\pi \leq p \leq \pi$.

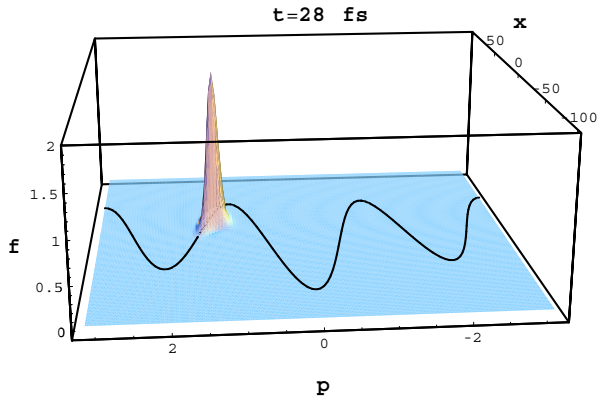

Figure 4: $f(x, p, t)$ at $t = 28$ fs, $-100 \leq x \leq 100$, $-\pi \leq p \leq \pi$.

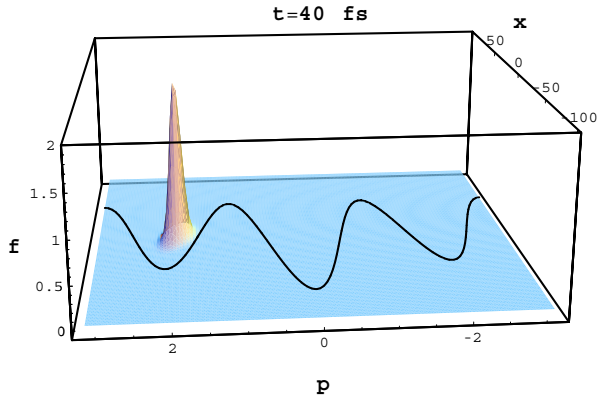

Figure 5: $f(x, p, t)$ at $t = 40$ fs, $-100 \leq x \leq 100$, $-\pi \leq p \leq \pi$.